Appl. Phys. B (2015) 118:253–259
DOI 10.1007/s00340-014-5980-1

Applied Physics B
Lasers and Optics

High-energy all-solid-state sodium beacon laser with line width of 0.6 GHz

Yan-Hua Lu · Gang Xie · Lei Zhang · Guo-Bin Fan · Yu Pang · Nan Li · Bin Wei · Song-Xin Gao · Wei Zhang · Chun Tang

Received: 19 October 2014 / Accepted: 8 December 2014 / Published online: 17 December 2014

Abstract A high-energy all-solid-state sodium beacon laser at 589 nm with a repetition rate of 50 Hz is introduced, which is based on sum frequency mixing between a 1,064 nm laser and a 1,319 nm laser. The 1,064 nm laser, which features an external modulated CW seed laser and several stages of amplifiers, can provide pulse energy of 740 mJ with ultra-narrow line width (~17 kHz) and superior stability. The 1,319 nm laser can deliver pulse energy of 580 mJ with a narrow line width of 0.6 GHz. By sum frequency mixing in a LBO crystal, pulse energy of 380 mJ is achieved at 589 nm with a conversion efficiency of 29 %. By controlling the center wavelength of 1,064 nm laser, the target beam's central wavelength is locked to be 589.1592 nm with a line width of 0.6 GHz, which is dominated mainly by the 1,319 nm laser. The beam quality factor is measured to be $M^2 = 1.6$. The pulse duration is measured to be 140 μs in full-width at half-maximum (FWHM). To the best of our knowledge, this represents the highest pulse energy for all-solid-state sodium beacon laser ever reported.

1 Introduction

Artificial laser beacons, which are commonly known as laser guide stars and can cover larger fraction of sky than natural stars in adaptive optics, have some significant applications [1, 2]. A laser, tuned to the D_{2a} resonance line of sodium atoms (589.159 nm), can create a beacon (i.e., sodium beacon) at an altitude of about 90 km. The development of adaptive optics on large-aperture astronomical telescopes demands compact sodium beacon lasers with high brightness to detect and correct the atmosphere wave front aberration.

Currently, there are mainly five methods to develop sodium beacon lasers. The first one is dye lasers, which can emit at 589 nm directly [3, 4]. However, they are faded out gradually due to their huge volume and notorious reliability. Solid-state lasers, as the second-generation sodium beacon lasers, are usually based on sum frequency mixing between 1,064 and 1,319 nm Nd:YAG lasers [5–7]. In the recent years, fiber lasers are growing as a competitive candidate for 589 nm sodium beacon laser, and there are usually two ways: one is based on sum frequency generation of 938 and 1,583 nm fiber lasers [8], and the other is based on the second harmonic generation of the 1,178 nm Raman fiber laser [9]. In addition, with the development of new laser technologies and laser materials, optical pumped semiconductor lasers (OPSLs) [10] and alkali vapor lasers [11] are also regarded as feasible methods to generate sodium lasers.

Among all these lasers, solid-state lasers and fiber lasers are most popular. However, in terms of pulse energy, solid-state laser is more powerful. To date, CW solid-state sodium beacon lasers, whose maximum power has achieved more than 50 W [5, 6, 9], have already been successfully supplied in astronomical adaptive optics. While to avoid temporal overlap with backwards Rayleigh scattering light in the lower atmosphere, pulsed sodium beacon lasers would be of greater significance [12, 13]. Furthermore, to get enough photons return without saturation during the

Y.-H. Lu (✉) · G. Xie · L. Zhang · G.-B. Fan · Y. Pang · N. Li · B. Wei · S.-X. Gao · W. Zhang · C. Tang
The Key Laboratory of Science and Technology on High Energy Laser, Institute of Applied Electronics, China Academy of Engineering Physics, Mianyang 621900, Sichuan, China
e-mail: happyeleo@163.com

G. Xie
e-mail: eyesopen@126.com

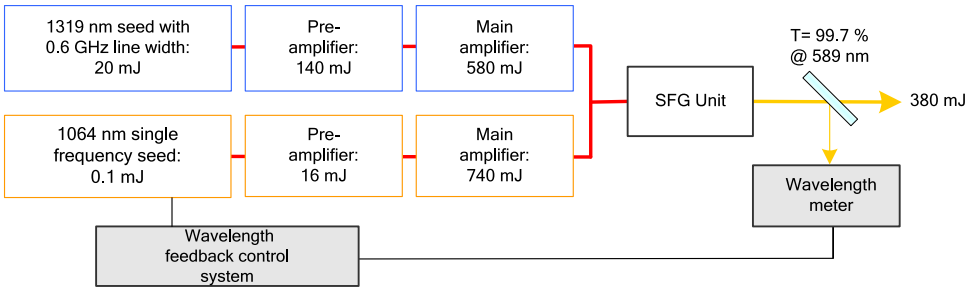

Fig. 1 Schematic of the sodium beacon laser

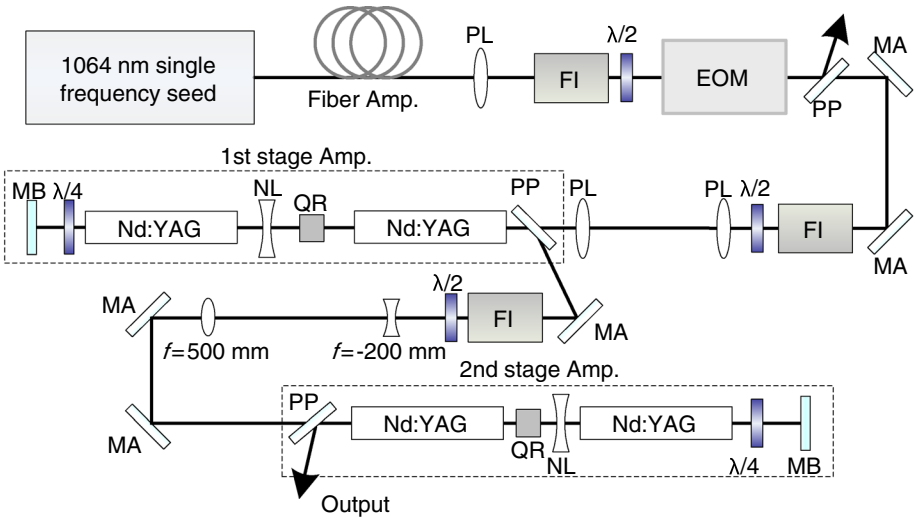

Fig. 2 Schematic of 1,064 nm single-frequency pulsed laser

seasons, in which the atoms column density of mesosphere sodium layer changes dramatically, lasers with several hundred mJ pulse energy, 100 μs level pulse width and several hundred MHz line width are called for in some special systems [14]. In the early 1990s, researchers in Lincoln Laboratory had developed a 500 mJ, 10 Hz,100 μs laser and a 24 mJ, 840 Hz, 60 μs solid-state laser pumped by flash lamps [15] with the line width of 1.5–3.0 GHz. With the development of pumping diode lasers, all-solid-state pulsed sodium beacon lasers have been widely spread [16, 17]. However, the performance, especially in terms of pulse energy, is still not so satisfactory.

In this letter, we report an all-solid-state, 380 mJ, sub-GHz line width 589 nm sodium beacon laser, which is generated by sum frequency mixing between a 1,064 nm laser and a 1,319 nm laser in a LBO crystal. The central wavelength and line width of the sodium beacon laser are dominated by the 1,064 nm laser and the 1,319 nm laser, respectively. Concretely, the 1,064 nm laser features an external modulated CW fiber laser seed (NKT Photonics Y10), so it is very easy to tuning its center wavelength, of which the tuning range is 0.7 nm with the temperature tuning accuracy of about 0.023 nm/°C. And then, the center wavelength of the sodium beacon laser can be regulated. While the line width is dominated mainly by the 1,319 nm laser's line width, because the 1,064 nm laser's line width is so narrow (~17 kHz), compared with that of the 1,319 nm laser's (0.6 GHz), it can be ignored. The two control loops are independent, and there is no cross talk which usually occurs in the wavelength tuning of the MLM lasers. Therefore, both the central wavelength and the line width can be reliably controlled.

2 Experimental setup and results

The schematic diagram for the high-energy all-solid-state sodium beacon laser is shown in Fig. 1. The laser consists of a 1,064 nm laser with the pulse energy of 740 mJ, a 1,319 nm laser with the pulse energy of 580 mJ, a sum frequency generation (SFG) unit and a wavelength feedback control system. Both of the 1,064 and 1,319 nm lasers take the structure of the master oscillator power-amplifier (MOPA). In the SFG unit, the 589 nm laser is generated by frequency mixing of the two infrared lasers. The central wavelength of the 589 nm sum frequency laser is finally locked to the sodium D_{2a} absorption line through the servo control of the 1,064 nm seed in close loop in the wavelength feedback control system.

The 1,064 nm laser is a single-frequency pulsed laser with a pulse width of 100 μs level and a vacuum central wavelength at 1,064.655 nm. As shown in Fig. 2, the whole experimental system is composed of a 1,064 nm seed laser, preamplifier (first-stage amplifier) and a main amplifier (second-stage amplifier). Different from the traditional pulsed laser technologies, the 1,064 nm pulsed seed laser is generated by external modulation of a continuous-wave (CW) single-frequency fiber laser through an electro-optic modulator (EOM). The 10 mW CW single-frequency seed is boosted to 700 mW by a fiber amplifier (Fiber Amp.). Then, it is collimated by a positive lens (PL, $f = 200$ mm), isolated by a Faraday isolator (FI) and modulated by a free-space EOM. PP is a polarizer plate and MA is a 45° high-reflection plane mirror at 1,064 nm. The modulated laser has a rectangle pulse shape with 50 Hz repetition rate, 200 μs pulse width, 0.1 mJ pulse energy and excellent beam quality, $M^2 < 1.1$ (all of the M^2 factor are measured by the Spiricon M2-200 beam propagation analyzer in the paper). The pulsed seed laser is then beam-expanded by two PLs (with the focal length of 150 and 300 mm, respectively) and power-amplified by two stages of Nd:YAG rods amplifiers.

The first-stage amplifier consists of two 25 Bar (5 sides by 5 circles) diode pump modules with a double-passes configuration, and MB is a 0° high-reflection plane mirror at 1,064 nm. The peak pump power of each module is 2.5 kW with a pump width of 250 μs. A quartz rotator (QR) and a negative lens (NL, $f = -400$ mm) are inserted between the two Nd:YAG rods (with a diameter of 4 mm and a length of 96 mm, 0.6 % doping) to compensate for the depolarization and the thermal lens effect. The pulse energy of 1,064 nm laser is 16 mJ, and the beam quality M^2 is about 1.2 after the first-stage amplifier. The second-stage amplifier is similar to the first one. The difference is that the gain modules are two 108 Bar (9 sides by 12 circles) diode pump modules with the diameter of 10 mm and the length of 190 mm of the Nd:YAG rods and peak pump power of 7.56 kW. The focal length of the NL between the modules is −1,300 mm. The final amplified energy is 740 mJ with the beam quality $M^2 = 1.8$. The estimated optical-to-optical efficiency is about 19 %. The pulse shape is modified to be trapezium with a pulse width of 150 μs in FWHM, as shown in Fig. 3.

Remarkably, there is no obvious line width broadening in the MOPA system. The line width is measured by the delayed self-heterodyne interferometer (DSHI) method [18]. The delayed line is a 10 km fiber. The measured results show that the lasers from the 1,064 nm CW seed laser, the fiber amplifier and the rod amplifiers have the similar line width characteristic. Figure 4 shows the line width of the 1,064 nm output laser and the central frequency of the x-axis in the figure is 70 MHz after an acusto-optic frequency shifter with the span range of the x-axis of 1 MHz. The -3-dB bandwidth of the beat spectrum of the amplified 1,064 nm laser is 34 kHz. Then, we can conclude that the actual line width of 1064 nm laser is about 17 kHz, limited by the precision of our measuring system.

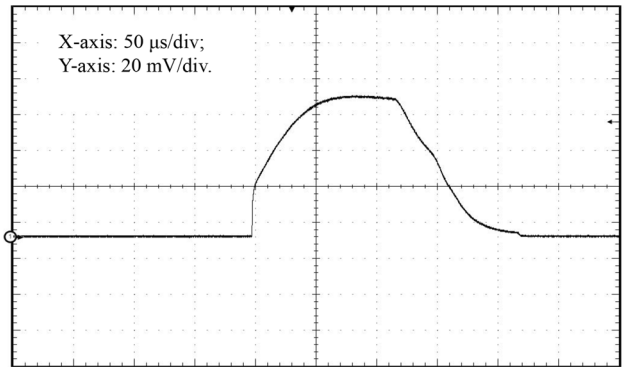

Fig. 3 Temporal pulse profile of the 1,064 nm laser after the two-stage amplifiers

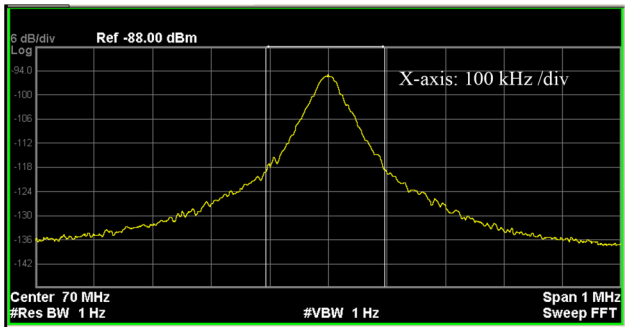

Fig. 4 Line width of the 1,064 nm output laser

The schematic for the 1,319 nm laser is shown in Fig. 5. It is quite similar to the 1,064 nm laser and it is composed of a 1,319 nm oscillator, a preamplifier (first-stage amplifier) and a main amplifier (second-stage amplifier). The 1,319 nm oscillator generates stable pulsed seed laser with 100 μs level pulse width. The oscillator is designed as a plano–plano cavity. Two Nd:YAG pumping modules with peak pump power of 1.5 kW are positioned symmetrically in the cavity. The diameter of each Nd:YAG rod is 2 mm, and a quartz rotator (QR) is inserted between the two rods. To improve the beam quality, a negative lens (NL, $f = -200$ mm) is inserted between the modules to enlarge the volume of the fundamental mode. Two etalons with thickness of 1.5 and 10 mm (with the free spectra range of 69 GHz and 10 GHz), coated with the reflectivity of 60 % in both sides, are introduced to narrow the line width and tune the central wavelength precisely. The special

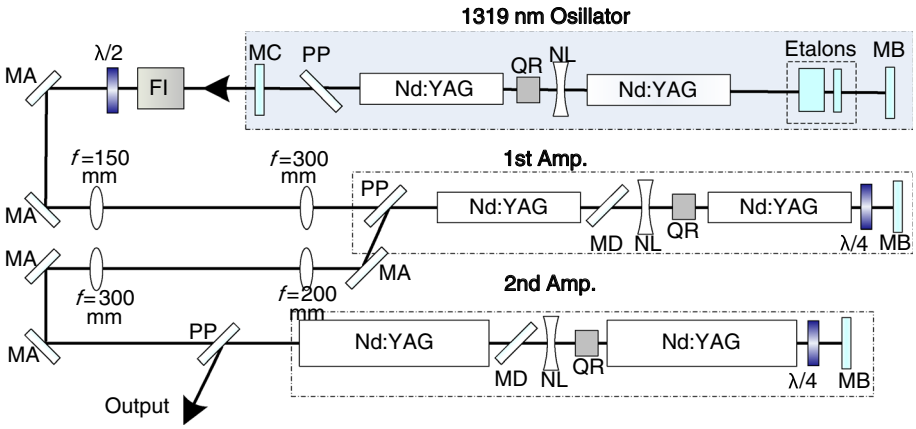

Fig. 5 Schematic of 1,319 nm MLM pulsed laser

anti-reflection (AR) coating at 1,064 nm of the 1,319 nm 0° high-reflection plane mirror (MB) and AR coating at 1,338 nm of the 1,319 nm 0° output mirror with the reflection of 60 % (MC) can suppress the laser oscillation at these two wavelengths and favor the 1,319 nm laser oscillation. The output pulse energy from oscillator is 20 mJ with $M^2 < 1.1$ and the linear polarization. The pulse width is 120 μs (in FWHM), and the line width is 0.6 GHz.

The 1,319 nm power-amplifiers also include two stages of amplifiers. Each amplifier works at 50 Hz repetition rate and 250 μs pulse width. The first-stage amplifier consists of two diode pump modules with 4.0 kW peak pumping power. The diameter of the gain medium (Nd:YAG crystal rod) is 4 mm and the length is 190 mm. The diodes of each module are arrayed in 5 sides by 10 circles. A 45° mirror (MD), coated AR at 1319 nm and high-reflection at 1,064 nm is inserted into the amplifier to prevent the 1,064 nm laser from oscillating. The focal length of the NL between the modules is −350 mm. While the total pumping energy is 2,000 mJ, the output energy of the first-stage amplifier is about 140 mJ, which means an optical-to-optical efficiency of about 6.0 % and an energy gain of 7.0. The second-stage amplifier is basically the same as the first-stage amplifier. Differently, it consists of two modules with the peak pumping laser of 8.8 kW with the diameter of gain medium of 6 mm and the length of 160 mm. The diodes of each module are arrayed in 11 sides by 8 circles. The focal length of the NL between the modules is −500 mm. With a total pumping energy of 4,400 mJ, the output energy from the second-stage amplifier is about 580 mJ, which means a energy gain of 4.1. The optical-to-optical efficiency is about 9.8 % and the beam quality M^2 is about 1.5. The pulse width is 120 μs (in FWHM). Different from 1,064 nm laser, there are lots of temporal spikes because of relaxation oscillation, as shown in Fig. 6.

The central wavelength and line width of the 1,319 nm laser are controlled by the two etalons inside the 1,319 nm oscillator. It is easier to narrow the line width to less than

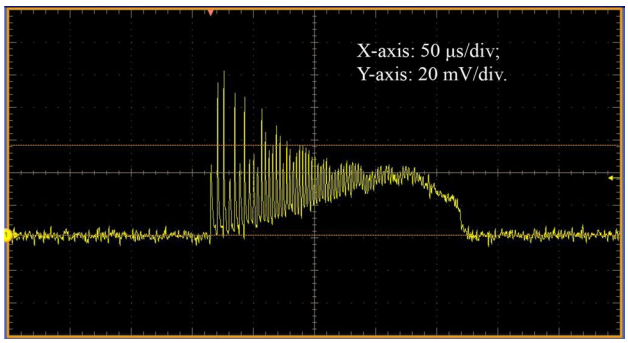

Fig. 6 Temporal pulse profile of the 1,319 nm output laser

1 GHz with two etalons instead of one. Both etalons are temperature-controlled by semiconductor coolers. The central wavelength can be tuned by changing the temperature of the etalons. Direct line width measurement at 1,319 nm is not possible by the wavelength meter (HighFinesse WS7). We convert the 1,319 nm laser to 659.5 nm light by the second harmonic generation. The measured vacuum central wavelength of the red laser is 659.57563 nm with a line width of about 1.25 GHz (corresponding to 1.82 pm), as shown in Fig. 7. For both the second harmonic generation and the sum frequency generation, the generated laser frequency can be described as [19]

$$\omega_3 = \omega_1 + \omega_2, \tag{1}$$

where ω_1 and ω_2 are the frequencies of the fundamental lasers.

Thus, by a differential, the line width of the generated laser frequency is represented as the sum of the line widths of the two laser frequencies with the form

$$\Delta\omega_3 = \Delta\omega_1 + \Delta\omega_2, \tag{2}$$

where $\Delta\omega_1$ and $\Delta\omega_2$ are the line widths of the fundamental lasers. For the second harmonic generation, ω_1 is equal to ω_2 and $\Delta\omega_1$ is equal to $\Delta\omega_2$.

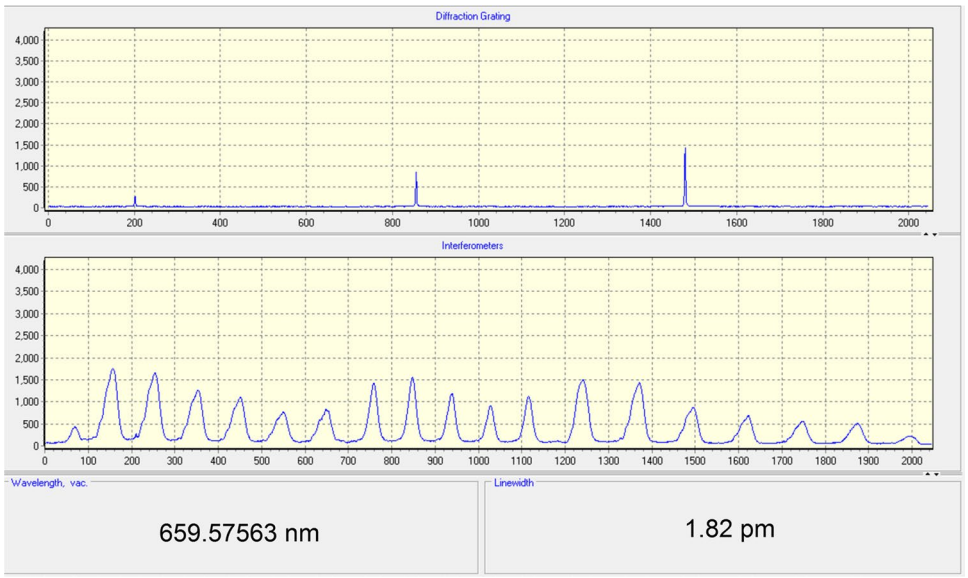

Fig. 7 Spectrum of the frequency-doubled laser of the 1,319 nm laser

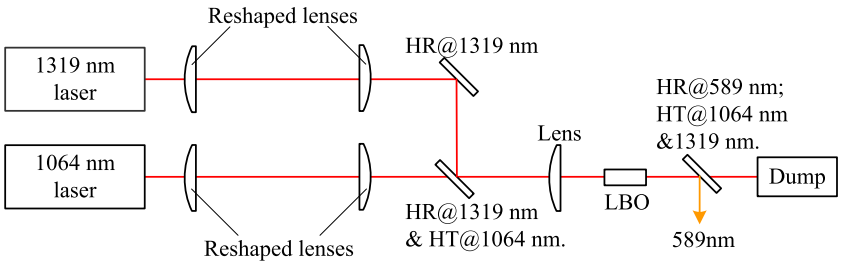

Fig. 8 Schematic of SFG system

Then, we can deduce that the central wavelength of 1,319 nm is 1,319.15126 nm with the line width of about 0.6 GHz.

The schematic of the SFG system is shown in Fig. 8. We use a LBO crystal to generate 589 nm sodium beacon laser from space-reshaped 1,064 nm laser and 1,319 nm laser. The LBO crystal is 4 mm × 4 mm × 50 mm in size and AR coated at 1,064, 1,319 and 589 nm. Its temperature is controlled within ± 0.1 °C by an oven working at 40.3 °C to enable non-critically phase-matched operation. To obtain efficient SFG conversion, the incident peak power density of 1,064 nm laser and 1,319 nm laser should be around 10 MW/cm^2. Therefore, the two laser beams need to be focused to the size of about 100 μm and overlapped well in space. We firstly use two lenses to reduce the diameters of 1,064 nm and 1,319 nm laser to be about Φ2.0 mm individually. The beams are then combined by a 45° dichromatic mirror. Finally, we focus the combined beams into the LBO crystal using a positive lens with $f = 240$ mm.

The frequency summing 589 nm laser's energy is measured, while the total energy of the fundamental lasers injected to the LBO crystal ranges from 100 mJ to 1.3 J, as shown in Fig. 9. While increasing the total incident pulse energy, the proportion of the 1,064 nm pulse energy to the

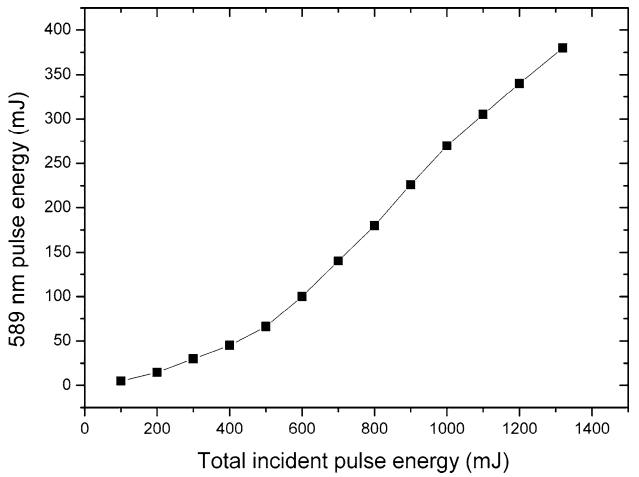

Fig. 9 589 nm laser pulse energy generated by frequency summing versus the total incident pulse energy of the fundamental lasers (just before they enter the LBO crystal)

1,319 nm pulse energy keeps about 1.27:1, which is near to the optimal photons ratio of 1:1. It is shown that the 589 nm pulse energy increases nonlinearly with the growing total incident pulse energy. When the total incident pulse energy

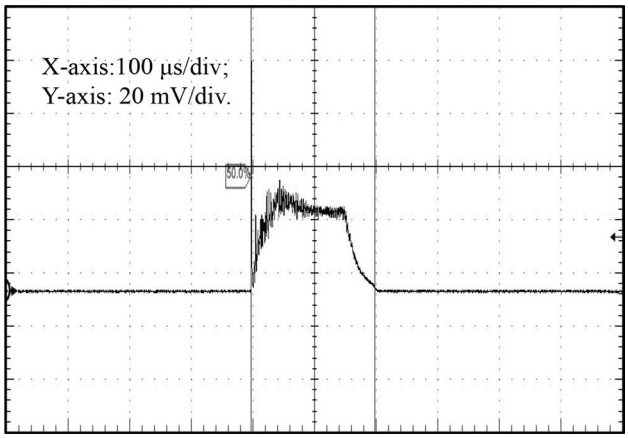

Fig. 10 Temporal pulse profile of the 589 nm output laser

is 100 mJ, we only get 5 mJ, 589 nm laser with an efficiency of 5 %. However, at the highest total incident fundamental laser energy of 1.3 J, the pulse energy of the 589 nm laser reaches to 380 mJ and the SFG efficiency is as high as 29 %. It is understandable that the SFG efficiency becomes higher due to the increasing power density of the fundamental lasers. The power stability at the highest output is measured to be 11.6 % (peak to peak in 20 min), and the beam quality M^2 factor is 1.6.

The pulse width is about 140 μs in FWHM, as shown in Fig. 10. It is noticeable that the 589 nm pulse wave shape is not accordant with that of either the 1,064 nm laser or the 1,319 nm laser. It has synthesized the temporal characteristics of the two lasers, and it is shown that the temporal spikes existed in 1,319 nm laser pulse become much less severe.

To lock the sodium beacon laser's central wavelength to the sodium D_{2a} line, the HighFinesse WS7 is used to read the central wavelength in real-time. Then, the 1,064 nm seed laser's central wavelength can be tuned by a PID controller. The result shows that the vacuum wavelength is locked to be around 589.1592 nm and the wavelength deviation (peak-to-peak value) in 20 min is 0.7 pm (about 600 MHz), as shown in Fig. 11.

From Eq. (2), the 589 nm laser's line width should be close to the sum of the line width of 1,064 nm laser and 1,319 nm laser in theory, if the phase mismatching and the line width broadening in LBO crystal are negligible. As shown in Figs. 4 and 7, the line width of the 1,064 nm laser (about 17 kHz) is much smaller than that (0.6 GHz) of the 1,319 nm laser. Therefore, it is deduced that line width of the 589 nm laser is about 0.6 GHz. The measured 589 nm line width is just about 0.6 GHz and equivalent to the sum of the two infrared lasers' line widths.

3 Conclusions

In conclusion, we have developed a high-energy, narrow-line-width, all-solid-state sodium beacon laser, which is based on the extra-cavity sum frequency generation between a 1,064 nm single-frequency laser and a 1,319 nm MLM laser. Both of the fundamental lasers take MOPA technologies, and the pulse energy of the 1,064 and 1,319 nm amplified lasers is 740 and 580 mJ, respectively. By sum frequency mixing in a LBO crystal, a 380 mJ, 589 nm laser has been obtained with the conversion efficiency of 29 %, the beam quality M^2 factor of 1.6 and the pulse width of 140 μs at the repetition rate of 50 Hz. With the feedback control of the center wavelength of 1,064 nm single-frequency seed laser, the sodium beacon laser's central wavelength has been locked to 589.1592 nm with a line width of 0.6 GHz, which is dominated mainly by the 1,319 nm MLM laser. The laser can find important applications in detecting and imaging in astronomy and will be used in the experimental research of pulsed sodium beacon photons return. Furthermore, we can apply the new spectra-controlling technology to get arbitrary value of the line width more easily in frequency summing lasers. With better thermal management and optimized laser cavity design, further improvements in pulse energy and line width as well as repetition rate are feasible.

Acknowledgments We are grateful for the support of the Science and Technology Development Fund of China Academy of Engineering Physics, 2012A0401020.

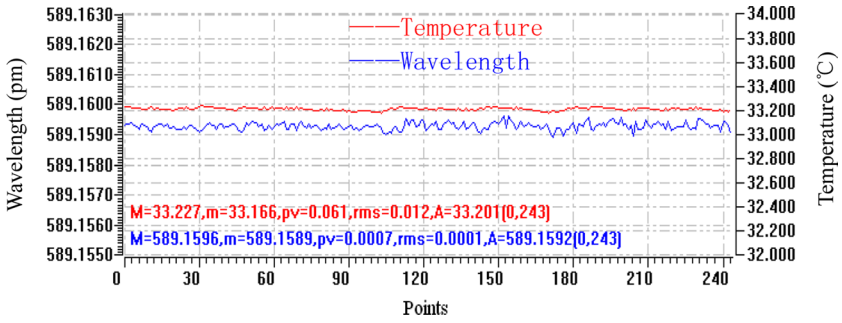

Fig. 11 Curve of 589 nm laser central wavelength

References

1. E.N. Ribak, Proc. SPIE **6272**, 62724E-1 (2006)
2. R. Joyce, C. Boyer, L. Daggert, B. Ellerbroek, E. Hileman, M. Hunten, M. Liang, Proc. SPIE **6272**, 62721H-1 (2006)
3. H.W. Friedman, Proc. SPIE **1859**, 251 (1993)
4. A. Quirrenbach, W. Hackenberg, H. Holstenberg, N. Wilnhammer, SPIE **3126**, 35 (1997)
5. A. Denman, P.D. Hillman, G.T. Moore, J.M. Telle, J.E. Preston, J.D. Drummond, R.Q. Fugate, Proc. SPIE **5707**, 46 (2005)
6. N. Saito, K. Akagawa, M. Ito, A. Takazawa, Y. Hayano, Y. Saito, M. Ito, H. Takami, M. Iye, S. Wada, Opt. Lett. **32**, 1965 (2007)
7. I. Lee, M. Jalali, N. Vanasse, Z. Prezkuta, K. Groff, J. Roush, N. Rogers, E. Andrews, G. Moule, B. Tiemann, A.K. Hankla, S.M. Adkins, C. d'Orgeville, Proc. SPIE **7015**, 70150N-1 (2008)
8. M. Pennington, J.W. Dawson, R.J. Beach, A. Drobshoff, M. Messerly, S. Mitchell, A. Brown, S.A. Payne, Conference on lasers and electro-optics, 532 (2005)
9. L.R. Taylor, Y. Feng, D.B. Calia, Opt. Express **18**, 8540 (2010)
10. M. Fllahi, F. Li, Y. Kaneda, C. Hessenius, H. Hader, H. Li, J.V. Moloney, B. Kunert, W. Stolz, S.W. Koch, J. Murray, R. Bedford, IEEE Photonics Technol. Lett. **11**, 1700 (2008)
11. R. Cwynar, B. Mussler, M.K. Shaffer, B.V. Zhadanov, R.J. Knize, Eleventh annual directed energy symposium (2008)
12. J. Kibblewhite, F. Shi, SPIE **3353**, 300 (1998)
13. L.C. Bradley, J. Opt. Soc. Am. B **9**, 1931 (1992)
14. J.M. Telle, P.W. Milonni, P.D. Hillman, SPIE **3264**, 37 (1998)
15. T.H. Jeys, Lincoln Lab. J. **4**, 133 (1991)
16. R. Dekany, V. Velur, H. Petrie, A. Bouchez, M. Britton, A. Morrissett, R. Thicksten, M. Troy, C. Shelton, T. Troung, J. Roberts, G. Brack, T. Trinh, S. Bikkannavar, S. Guiwitz, J. Angione, F. Shi, and E. Kibblewhite, Amos Technical conference proceedings, (2005)
17. Z. Xu, S. Xie, Y. Bo, J. Zou, B. Wang, P. Wang, Z. Wang, Y. Liu, J. Xu, Q. Peng, D. Cui, Acta Opt. Sinica **31**, 0900111-1 (2011)
18. T. Okoshi, K. Kikuchi, A. Nakayama, Electron Lett. **16**, 630 (1980)
19. R.W. Boyd, *Nonlinear Optics*, 3rd edn. (Elsevier, Singapore, 2010)